

MOL #68577

**Activated Sterol Regulatory Element-Binding Protein-2 Suppresses Hepatocyte Nuclear  
Factor-4-Mediated *Cyp3a11* Expression in Mouse Liver**

**Shin-ichi Inoue, Kouichi Yoshinari, Mika Sugawara and Yasushi Yamazoe**

Division of Drug Metabolism and Molecular Toxicology, Graduate School of Pharmaceutical Sciences,

Tohoku University, 6-3 Aramaki-aoba, Aoba-ku, Sendai, Miyagi 980-8578, Japan (S.I., K.Y., M.S., Y.Y.)

MOL #68577

a) Running title: SREBP-2-mediated down-regulation of *Cyp3a11* expression

b) Corresponding author: Kouichi Yoshinari, Ph.D. Division of Drug Metabolism and Molecular

Toxicology, Graduate School of Pharmaceutical Sciences, Tohoku University, 6-3 Aramaki-aoba,

Aoba-ku, Sendai, Miyagi 980-8578, Japan. Telephone: +81-22-795-6828; FAX: +81-22-795-6826;

e-mail: [kyoshina@mail.pharm.tohoku.ac.jp](mailto:kyoshina@mail.pharm.tohoku.ac.jp)

c) The number of text pages 47

The number of tables 0

The number of figures 8

The number of references 37

The number of words Abstract 249

Introduction 694

Discussion 901

d) Abbreviations: SREBP, sterol regulatory element-binding protein; bHLH, basic helix-loop-helix;

LDL-R, low density lipoprotein-receptor; CYP, cytochrome P450; HNF-4 $\alpha$ , hepatocyte nuclear

factor-4 $\alpha$ ; DR1, direct repeat separated by mononucleotide; PGC-1 $\alpha$ , peroxisome

proliferator-activated receptor  $\gamma$  coactivator-1 $\alpha$ ; CAR, constitutive androstane receptor; PXR,

pregnane X receptor; BSA, bovine serum albumin; DTT, dithiothreitol; PMSF, phenylmethylsulfonyl

MOL #68577

fluoride; CD, conventional laboratory diet; LCD, low-cholesterol regular diet; NE, nuclear extract; h,  
human; m, mouse; DN, dominant negative; EMSA, electrophoretic mobility shift assay; GST,  
glutathione *S*-transferase; CHIP, chromatin immunoprecipitation; PEPCCK1, phosphoenolpyruvate  
carboxykinase 1; DBD, DNA binding domain; LBD, ligand binding domain. SDS, sodium dodecyl  
sulfate.

MOL #68577

## Abstract

Sterol regulatory element-binding protein-2 (SREBP-2) is a key transcription factor for the cholesterol homeostasis. Recent studies have suggested the association of CYP3A enzymes, major drug-metabolizing enzymes, with cholesterol metabolism. In the present study, we have investigated a possible involvement of SREBP-2 in hepatic *Cyp3a11* expression. Feeding a low-cholesterol diet (LCD) to mice activated hepatic SREBP-2 while it attenuated hepatic *Cyp3a11* expression. These phenomena were reversed by cholesterol supplementation to LCD. In reporter assays, the overexpression of constitutively active SREBP-2 reduced *Cyp3a11* reporter activity through the region from -1581 to -1570 of *Cyp3a11*. This region contained a putative hepatocyte nuclear factor-4 $\alpha$  (HNF-4 $\alpha$ )-binding motif, and HNF-4 $\alpha$ , but not SREBP-2, bound to the motif in *in vitro* binding assays. With the mutation or deletion of this motif, the SREBP-2-dependent suppression of *Cyp3a11* expression disappeared in reporter assays. In pull-down assays and co-immunoprecipitation assays, SREBP-2 bound to peroxisome proliferator-activated receptor  $\gamma$  coactivator-1 $\alpha$  (PGC-1 $\alpha$ ), a major coactivator for HNF-4 $\alpha$ , *via* its transactivation domain and inhibited the interaction between HNF-4 $\alpha$  and PGC-1 $\alpha$  *in vitro*. Consistently, a mutant SREBP-2 lacking the transactivation domain did not reduce *Cyp3a11* reporter activity. Furthermore, PGC-1 $\alpha$  overexpression relieved the SREBP-2-mediated reduction of *Cyp3a11* reporter activity. Finally, chromatin immunoprecipitation assays demonstrated that the extent of PGC-1 $\alpha$  binding to the *Cyp3a11* promoter

MOL #68577

was reduced by LCD-feeding in mouse livers. In conclusion, activated SREBP-2 interacts with PGC-1 $\alpha$  in mouse livers at reduced cholesterol intake. This results in the reduced PGC-1 $\alpha$  recruitment to HNF-4 $\alpha$  on the *Cyp3a11* promoter and the subsequent down-regulation of *Cyp3a11* expression.

MOL #68577

## Introduction

Sterol regulatory element-binding proteins (SREBPs) are transcription factors that play major roles in the regulation of cholesterol, triglyceride and fatty acid homeostasis. SREBPs are synthesized as membrane-bound endoplasmic reticulum proteins with two membrane-spanning domains (Brown and Goldstein, 1997; Horton et al., 2002). Newly synthesized premature SREBPs are associated with the SREBP cleavage-activating protein, a sterol-sensing molecule (Brown and Goldstein, 1997; Horton et al., 2002). When cellular sterol levels are low, SREBP cleavage-activating protein escorts SREBPs to the Golgi compartment, where SREBPs are processed sequentially by two proteases, designated site-1 and site-2 proteases (Brown and Goldstein, 1997; Horton et al., 2002). Proteolytic cleavage releases the transcriptionally active its N-terminal portion containing a DNA binding motif, basic helix-loop-helix (bHLH) leucine zipper (Brown and Goldstein, 1997; Horton et al., 2002). It enters the nucleus and binds to specific sterol regulatory elements in the promoters of cholesterologenic and lipogenic genes, thereby activating their transcription (Horton et al., 2002). Among three known SREBP isoforms (SREBP-1a, SREBP-1c and SREBP-2), SREBP-2 is constitutively expressed in various tissues, and, when activated, it up-regulates the expression of numbers of genes for cholesterol uptake and synthesis to maintain cellular cholesterol level. Its target genes include those encoding low density lipoprotein-receptor (LDL-R), 3-hydroxy-3-methylglutaryl-CoA synthase, 3-hydroxy-3-methylglutaryl-CoA reductase and squalene

MOL #68577

epoxidase (Brown and Goldstein, 1997; Horton et al., 2002).

Excess cellular cholesterol is converted into oxysterols and bile acids by multiple enzymes including cytochrome P450s (CYPs). A major human drug-metabolizing enzyme CYP3A4 and its mouse homologue CYP3A11 have been reported to be involved in this cholesterol metabolism. They catalyze the 4 $\beta$ -hydroxylation of cholesterol and mediate the formation of various intermediates in the bile acid synthetic pathway such as 5 $\beta$ -cholestane-3 $\alpha$ ,7 $\alpha$ ,12 $\alpha$ ,25-tetrol (Bodin et al., 2002; Bodin et al., 2001; Goodwin et al., 2003; Honda et al., 2001; Pikuleva, 2006). These suggest a distinct endogenous role of CYP3As in cholesterol homeostasis. However, the contribution of CYP3As to cholesterol homeostasis remains to be defined.

Hepatocyte nuclear factor-4 $\alpha$  (HNF-4 $\alpha$ ) is a highly conserved member of the nuclear receptor superfamily. HNF-4 $\alpha$  binds to a direct repeat with one or two nucleotide spacer (designated DR1 or DR2, respectively) as a homodimer and is involved in the expression of genes associated with a variety of liver functions, including CYP genes (Gonzalez, 2008; Jiang et al., 1995; Miyata et al., 1995). The expression of HNF-4 $\alpha$  antisense RNA in primary human hepatocytes dramatically decreased mRNA levels of *CYP3A4*, *CYP3A5*, *CYP2A6*, *CYP2B6*, *CYP2C9* and *CYP2D6* (Jover et al., 2001). Recently, we have also reported that mRNA levels of several CYP genes including *CYP3A4* were dramatically decreased in cultured human hepatocytes after the infection of the adenovirus expressing human HNF-4 $\alpha$ -small

MOL #68577

interfering RNA (Kamiyama et al., 2007). Furthermore, hepatic *Cyp3a* expression is greatly reduced in liver-specific HNF-4 $\alpha$  knock-out mice (Wiwi et al., 2004). These data indicate that HNF-4 $\alpha$  plays a dominant role in the expression of *CYP3A* genes in the liver.

The HNF-4 $\alpha$ -mediated gene transcription is cooperated with coactivators, such as peroxisome proliferator-activated receptor  $\gamma$  coactivator-1 $\alpha$  (PGC-1 $\alpha$ ) (Rhee et al., 2003; Yoon et al., 2001). PGC-1 $\alpha$  recruits chromatin-modifying enzymes having histone acetyltransferase activity, which opens the chromatin and promotes RNA polymerase II occupancy, resulting in the increased transcription of target genes (Monsalve et al., 2000; Puigserver et al., 1999). PGC-1 $\alpha$  interacts with numerous nuclear receptors, in addition to HNF-4 $\alpha$ , including peroxisome proliferator-activated receptor  $\alpha$ , constitutive androstane receptor (CAR) and pregnane X receptor (PXR) (Li and Chiang, 2005; Shiraki et al., 2003; Vega et al., 2000). These nuclear receptors regulate diverse biological functions, such as lipid, glucose and xenobiotic metabolism. Thus, PGC-1 $\alpha$  appears to be a convergence point of crosstalk between xenobiotic and other signaling pathways.

We have recently observed that hepatic *Cyp3a11* expression is attenuated in mice fed a high triglyceride-containing diet (Yoshinari et al., 2006). Given that the involvement of CYP3A enzymes in cholesterol metabolism is suggested, cellular cholesterol levels may affect CYP3A expression levels. In the present study, we have found for the first time that *Cyp3a11* expression is down-regulated in mouse



MOL #68577

livers by feeding a low-cholesterol diet, and investigated the role of SREBP-2 in this down-regulation. We here demonstrate that activated SREBP-2 inhibits the interaction of PGC-1 $\alpha$  with HNF-4 $\alpha$ , suppressing the HNF-4 $\alpha$ -mediated *Cyp3a11* expression in mouse liver.

MOL #68577

## Materials and Methods

### Materials

Streptavidin Magnetic Beads, T4 polynucleotide kinase and restriction enzymes were purchased from New England BioLabs (Ipswich, MA). Fetal bovine serum, pepstatin A and [ $\gamma$ - $^{32}$ P]ATP were purchased from BioWest (Nuaille, France), Peptide Institute (Minoh, Japan) and Perkin Elmer (Waltham, MA), respectively. Bovine serum albumin (BSA), cholesterol, dithiothreitol (DTT), leupeptin, phenylmethylsulfonyl fluoride (PMSF), spermidine, spermine, protease inhibitor cocktail and proteinase K were purchased from Sigma-Aldrich (St Louis, MO). All other chemicals were purchased from Wako Pure Chemical Industries (Osaka, Japan). Oligonucleotides were commercially synthesized by Fasmac (Atsugi, Japan).

### Animal treatment

Male C57BL/6N mice (7-week-old; Charles River Laboratories Japan, Yokohama, Japan) were maintained under a 12-hr light/12-hr dark cycle and fed a conventional laboratory diet (CD; CE-2, CLEA Japan, Tokyo, Japan) and water *ad libitum* for a week for acclimatization. Mice were then fed CD, a low-cholesterol regular diet (LCD; D12450BM, Research Diet, New Brunswick, NJ) or 2% cholesterol-supplemented LCD for 6 days. Composition of CD and LCD are shown in supplemental

MOL #68577

Tables S1 and S2. CD and LCD contains in 0.1% and 0.0056% of cholesterol, respectively (data obtained from CLEA Japan and Research Diet). The animal experiment was approved by the Animal Care and Use Committee of Tohoku University.

### Preparation of nuclear extracts

Mouse liver was pooled for each diet group (n=6 or 7), homogenized in homogenization buffer (10 mM HEPES-KOH, pH 7.6, 2 M sucrose, 25 mM KCl, 0.15 mM spermidine, 0.5 mM spermine, 1 mM EDTA, 10% glycerol) and centrifuged at 20,000 rpm for 30 min at 4°C with a swing rotor (P40ST-1308; Hitachi koki, Tokyo, Japan). The precipitate was suspended in 10 mM HEPES-KOH, pH 7.6, 0.1 M KCl, 3 mM MgCl<sub>2</sub>, 0.1 mM EDTA, 1 mM Na<sub>3</sub>VO<sub>4</sub>, 10% glycerol, 1 µg/ml pepstatin A, 1 µg/ml leupeptin, 0.1 mM PMSF, 1 mM DTT. After addition of NaCl to make final salt concentration of 400 mM, the suspension was incubated at 4°C for 30 min and centrifuged at 20,000×g for 20 min at 4°C. The supernatant was dialyzed against 20 mM HEPES-KOH, pH 7.6, 0.1 M KCl, 0.2 mM EDTA, 1 mM Na<sub>2</sub>MoO<sub>4</sub>, 20% glycerol, 1 µg/ml pepstatin A, 1 µg/ml leupeptin, 0.1 mM PMSF, 1 mM DTT. Nuclear extracts (NEs) were subjected to immunoblotting with anti-SREBP-2 (10007663; Cayman Chemical, MI) antibody. The band intensities were quantified using NIH image software.

MOL #68577

### Determination of protein concentration

The protein concentration was determined by Bradford method with Bio-Rad Protein Assay (Bio-Rad Laboratories, Hercules, CA) with BSA as standard.

### Quantitative reverse transcription-PCR

Total liver RNA was extracted using the acid guanidine thiocyanate-phenol-chloroform method and cDNA was synthesized using High-Capacity cDNA Reverse Transcription Kit (Applied Biosystems, Foster City, CA). Quantitative PCR was performed using Power SYBR Green PCR Master Mix (Applied Biosystems) with Thermal Cycler Dice Real Time System TP800 (Takara Bio, Otsu, Japan). The sequences of the primers used are shown in supplemental Table S3.

### Plasmid preparation

*Cyp3a11* luciferase reporter constructs were prepared by inserting *Cyp3a11* promoter DNA, which were amplified by PCR using TaKaRa Ex Taq (Takara Bio) or KOD FX (TOYOBO, Osaka, Japan) with mouse genomic DNA as a template, into Acc65I and XhoI sites of pGL4.10 (Promega, Madison, WI). A mutation construct was made by using QuikChange Lightning Site-Directed Mutagenesis Kit (Stratagene, LaJolla, CA) with the primers,

MOL #68577

5'-CACAAATTGCAGGGTAGATGATATCAGCTAATGAGTTACCCTTTCTCAGGACTGTAAATATT

AGCAATCATTCTGTGA-3' and 5'-

TCACAGAATGATTGCTAATATTTACAGTCCTGAGAAAGGGTAACTCATTAGCTGATATCATCTAC

CCTGCAATGTTGTG-3'. cDNAs of nuclear forms of human (h) and mouse (m) SREBP-2, hHNF-4 $\alpha$

and mHNF-4 $\alpha$ , dominant negative (DN) forms of hSREBP-2 and mSREBP-2, mSREBP-2DN-2 and

nuclear form of mSREBP-1a were amplified by PCR and inserted into pTarget (Promega). The fragments

obtained by digesting the pTarget expression plasmids with MluI and NotI and hPGC-1 $\alpha$  cDNA fragment

obtained by digesting pcDNA3/HA-hPGC-1 $\alpha$  (gift of Dr. Anastasia Kralli) with KpnI and NotI were

inserted into the same restriction sites of pT<sub>N</sub>T (Promega). Primers used for PCR are shown in

supplemental Tables S4 and S5.

## Reporter assay

HepG2 (RIKEN Bio Resource Center, Tsukuba, Japan) were maintained as described previously (Yoshinari et al., 2010). The cells were seeded in 24-well plates (BD Biosciences, Heidelberg, Germany) at  $5 \times 10^4$  cells/well 24 hr before transfection. Reporter construct and pTarget expression plasmid were cotransfected using calcium phosphate method. pSV- $\beta$ -galactosidase Control Vector (Promega) was cotransfected to normalize transfection efficiency. Eight hr after transfection, medium was changed and

MOL #68577

the cells were cultured in Dulbecco's modified Eagle's medium supplemented with 10% fetal bovine serum for additional 40 hr. Subsequently, the cells were harvested, and luciferase and  $\beta$ -galactosidase activities were determined as described previously (Yoshinari et al., 2010).

### Electrophoretic mobility shift assay

Electrophoretic mobility shift assay (EMSA) was performed as previously described (Toriyabe et al., 2009). hHNF-4 $\alpha$  was synthesized *in vitro* with the pT<sub>N</sub>T plasmid containing hHNF-4 $\alpha$  cDNA using T<sub>N</sub>T SP6 Quick Coupled Transcription/Translation System (Promega). The probe sequences are shown in Fig. 3B. Supershift reaction was performed with anti-HNF-4 $\alpha$  antibody (sc-6556X; Santa Cruz Biotechnology, Santa Cruz, CA).

### Preparation of DR1-affinity resin

Oligonucleotides (5'-ACTGTAATGAGGGCAAAGTTCTCAGG-3' and 5'-CAGTCCTGAGAACTTTGCCCTCATTA-3') corresponding to *Cyp3a11* DR1 were annealed and phosphorylated with T4 polynucleotide kinase. After purification with Wizard SV Gel and PCR Clean-Up System (Promega), they were self-ligated using T4 DNA ligase (Takara Bio), labeled with biotin-14-dATP (Invitrogen) using Klenow fragment (Takara Bio), and purified as described above. The

MOL #68577

biotin-labeled oligonucleotides were incubated with Streptavidin Magnetic Beads to obtain DR1-affinity resin.

#### DR1-affinity assay

mHNF-4 $\alpha$ , mSREBP-2 and hPGC-1 $\alpha$  were synthesized *in vitro* as described above. Reaction mixture (200  $\mu$ l), containing DR1-affinity resin, 20 mM HEPES-KOH, pH 7.6, 0.8  $\mu$ g of salmon sperm DNA (BioDynamics Laboratory, Tokyo, Japan), 0.1% Nonidet P-40 (Nacalai tesque, Kyoto, Japan), 0.1 M KCl, 0.2 mM EDTA, 20% glycerol and 10  $\mu$ l *in vitro* synthesized proteins, was incubated at 4°C for 30 min. The supernatant after centrifugation was kept as an unbound fraction. The resin was washed with 20 mM HEPES-KOH, pH 7.6, 0.1 M KCl, 0.2 mM EDTA, 1 mM Na<sub>2</sub>MoO<sub>4</sub>, 20% glycerol and bound proteins were eluted successively with 25 mM Tris-HCl, pH 8.0, 0.5 mM EDTA, 0.5 mM DTT, 10% glycerol, 0.05% Nonidet P-40 containing 0.1 M, 0.5 M or 1 M NaCl. Eluates and unbound fractions were subjected to immunoblotting with anti-SREBP-2 (Cayman Chemical), anti-HNF-4 $\alpha$  (Santa Cruz Biotechnology) or anti-PGC-1 $\alpha$  (sc-13067; Santa Cruz Biotechnology) antibody.

#### GST pull-down assay

A series of the cDNA fragments of mHNF-4 $\alpha$  or hSREBP-2 were inserted into pGEX-4T-1 (GE

MOL #68577

Healthcare, Buckinghamshire, UK). Primers used are shown in supplemental Table S6. Glutathione *S*-transferase (GST), a series of GST-HNF-4 $\alpha$  and GST-SREBP-2 were expressed in BL21(DE3)pLysS (Novagen, Darmstadt, Germany), Origami2(DE3) (Novagen) or Rosetta-gami(DE3)pLysS (Novagen) and purified with glutathione-Sepharose 4B (GE Healthcare). mSREBP-2, mSREBP-2DN, mSREBP-2DN-2 and mSREBP-1a were synthesized *in vitro* as described above. Glutathione-Sepharose 4B was incubated with 20  $\mu$ g of GST, GST-HNF-4 $\alpha$  or GST-SREBP-2 in binding buffer (50 mM Tris-HCl, pH 8.0, 34 mM NaCl, 1 mM EDTA) at 4°C for 1 hr and washed three times with the same buffer. Protein-bound beads were incubated with 10  $\mu$ l of each *in vitro* synthesized protein at room temperature for 1 hr in binding buffer. The supernatant after centrifugation was kept as an unbound fraction. In competition assays using oligonucleotides, various amounts (4, 133 or 400 pmol) of oligonucleotides (Fig. 3B) were added to the reaction before the addition of mSREBP-2. In competition assays using *in vitro* synthesized proteins, hSREBP-2- or hSREBP-2DN-containing lysate (10 or 30  $\mu$ l), synthesized *in vitro* as described above, was added to the reaction before the addition of PGC-1 $\alpha$  lysate. The beads were washed five times with binding buffer and bound proteins were eluted with Sample buffer (31 mM Tris-HCl, pH 6.8, 1% SDS, 5% sucrose, 0.1  $\mu$ g/ $\mu$ l bromophenol blue, 5% 2-mercaptoethanol) and subjected to immunoblotting with anti-SREBP-2 (Cayman Chemical), anti-PGC-1 $\alpha$  (Santa Cruz Biotechnology) or anti-SREBP-1a (NB100-2215SS, Novus Biologicals, Littleton, CO) antibody.



MOL #68577

### Co-immunoprecipitation assay

NEs of mouse livers (0.6 mg) were precleared by incubation with 50  $\mu$ l of protein G-coupled Dynabeads (Invitrogen) at 4°C for 3 hr. The precleared samples were divided into 2 tubes (0.3 mg each) and subjected to immunoprecipitation at 4°C overnight with 5  $\mu$ g of normal rabbit IgG (Millipore, Billerica, MA) or anti-SREBP-2 antibody (Cayman Chemical). The immune complexes were incubated with protein G-coupled Dynabeads (50  $\mu$ l) at 4°C for 2 hr. The beads were washed five times in 20 mM HEPES-KOH, pH 7.6, 100 mM NaCl, 1 mM EDTA. The immune complexes were eluted with Sample buffer and subjected to immunoblotting with anti-SREBP-2 (1/3 of the eluates; Cayman Chemical) and anti-PGC-1 $\alpha$  antibody (2/3 of the eluates; Santa Cruz Biotechnology).

### Chromatin immunoprecipitation assay

Pooled mouse livers (0.2 g; n=6 or 7) were minced and crosslinked in 1% formaldehyde at room temperature for 5 min. The crosslinking was stopped by adding glycine at final concentration of 125 mM. After 5-min incubation at room temperature, the liver was collected by centrifugation, homogenized in homogenization buffer used for NE preparation containing protease inhibitor cocktail, and centrifuged at 20,000 rpm for 30 min at 4°C with a swing rotor. The precipitate was suspended in ChIP lysis buffer (50

MOL #68577

mM Tris-HCl, pH 8.0, 1% SDS, 10 mM EDTA) and sonicated with Bioruptor (UCD-250; Cosmo Bio, Tokyo, Japan) at the middle setting of power output for 15 sec 12 times with 45-sec interval. An aliquot was saved as input sample. After centrifugation, the supernatant was diluted 10 times with 50 mM Tris-HCl, pH 8.0, 150 mM NaCl, 1% Triton X-100, 0.1% sodium deoxycholate. After addition of BSA (100  $\mu$ g), salmon sperm DNA (10  $\mu$ g) and 50  $\mu$ l of protein G-coupled Dynabeads, samples were incubated at 4°C for 3 hr. The precleared samples were divided into 5 tubes and subjected to immunoprecipitation at 4°C overnight with 6  $\mu$ g of normal goat IgG (sc-2028; Santa Cruz Biotechnology), normal rabbit IgG (NI01; Merck, Darmstadt, Germany), anti-HNF-4 $\alpha$  (Santa Cruz Biotechnology), anti-SREBP-2 (Cayman Chemical) or anti-PGC-1 $\alpha$  (516557; Merck) antibody. The immune complexes were incubated with protein G-coupled Dynabeads (50  $\mu$ l) at 4°C for 2 hr. The beads were washed five times with 50 mM HEPES-KOH, pH 7.55, 500 mM LiCl, 1 mM EDTA, 1% Nonidet P-40, 0.7% sodium deoxycholate and once with 10 mM Tris-HCl, pH 8.0, 1 mM EDTA, 50 mM NaCl. The immune complexes were eluted by incubation in CHIP lysis buffer at 65°C for 30 min. The supernatant after centrifugation was incubated at 65°C for 6 hr to decrosslink. After addition of 80  $\mu$ g of RNase A (Nacalai Tesque), samples were incubated at 37°C for 30 min. Proteins were then digested with proteinase K (80  $\mu$ g) at 55°C for 1 hr. DNA samples were purified with Wizard SV Gel and PCR Clean-Up System and used as a template for PCR with Takara Ex Taq Hot Start Version (Takara Bio) and primers (Table S7).

MOL #68577

## Statistical analysis

One-way analysis of variance with Dunnett's post-hoc test was performed using Prism software version 4.0 (GraphPad Software, San Diego, CA).

MOL #68577

## Results

Influence of dietary cholesterol levels on *Cyp3a11* expression and SREBP-2 function in mouse liver.

To verify the effects of dietary cholesterol on hepatic *Cyp3a11* expression, mice were fed CD, LCD or 2% cholesterol-supplemented LCD for 6 days, and hepatic *Cyp3a11* mRNA and CYP3A11 protein levels were determined. Hepatic *Cyp3a11* mRNA levels in LCD-fed mice were significantly lower than those in CD-fed mice, and the supplementation of LCD with 2% cholesterol significantly reversed the mRNA levels (Fig. 1A). Similarly, hepatic CYP3A11 protein levels were substantially lower in LCD-fed mice than in CD-fed mice, and increased by the cholesterol supplementation to LCD (Fig. S1). These results suggest a possible association of the reduced nutritional intake of cholesterol with the down-regulation of *Cyp3a11* expression in mouse livers.

SREBP-2 is activated under conditions of low cellular cholesterol to maintain cholesterol levels. As expected, hepatic nuclear SREBP-2 levels determined by immunoblotting markedly higher in LCD-fed mice than in CD-fed mice and mice fed cholesterol-supplemented LCD (Fig. 1B). The protein levels in LCD-fed mice and 2% cholesterol-supplemented LCD-fed mice were about 271% and 71% that of CD-fed mice, respectively. Consistently, hepatic mRNA levels of SREBP-2-responsive genes, *Srebf2* (SREBP-2), *Ldlr* (LDL-R), *Hmgcs1* (3-hydroxy-3-methylglutaryl-CoA synthase 1) and *Sqle* (squalene epoxidase) were also significantly higher in LCD-fed mice than in CD-fed mice, and the cholesterol

MOL #68577

supplementation to LCD reduced the mRNA levels (Fig. 1A).

### SREBP-2-dependent suppression of *Cyp3a11* transcription

To examine the influence of SREBP-2 on *Cyp3a11* transcription, reporter assays were performed using the constructs containing various *Cyp3a11* 5'-flanking regions and expression plasmid of SREBP-2 nuclear form. The insertion of 8.9 kb, 3.5 kb, 2 kb or 1 kb of the *Cyp3a11* promoter increased reporter activities, and the overexpression of active SREBP-2 reduced their reporter activities except for the construct containing the region from -998 to +47 (Fig. 2A). To identify the region responsible for the SREBP-2-dependent suppression of *Cyp3a11* expression, detailed assays were performed with another sets of reporter constructs. The deletion of the region from -1581 to -1524 resulted in complete loss of the SREBP-2-mediated suppression of *Cyp3a11* expression (Fig. 2B and 2C).

### Binding of HNF-4 $\alpha$ to the DR1 motif in *Cyp3a11*.

To identify a transcription factor(s) that binds to the region from -1581 to -1524 of *Cyp3a11*, the web-based program TESS (Transcription Element Search System; <http://www.cbil.upenn.edu/tess>) was used. The analysis revealed that there was no sterol regulatory element in this region. Instead, a putative HNF-4 $\alpha$  binding motif, the direct repeat separated by a nucleotide or DR1, was found (Fig. 3A). To

MOL #68577

examine the direct binding of HNF-4 $\alpha$  to the DR1 motif, we performed EMSAs with radio-labeled oligonucleotides (Fig. 3B) and *in vitro* synthesized proteins. CYP7A1 and phosphoenolpyruvate carboxykinase 1 (PEPCK1) probes containing known HNF-4 $\alpha$  binding motifs (Miao et al., 2006; Yamamoto et al., 2004) were used as positive controls. HNF-4 $\alpha$  bound to DR1 probe as well as CYP7A1 and PEPCK1 probes but not mutated probe DR1mt, and the addition of anti-HNF-4 $\alpha$  antibody supershifted the HNF-4 $\alpha$ -DR1 complex (Fig. 3C). The binding specificity of HNF-4 $\alpha$  to DR1 probe was confirmed by competition with unlabeled DR1 or PEPCK1 probe but not with DR1mt probe (Fig. S2A). In contrast, SREBP-2 bound to LDL-R probe, containing a known SREBP-2 binding motif (Yamamoto et al., 2004), but not to DR1 probe (Fig. S2B).

The binding of HNF-4 $\alpha$  to the DR1 motif was further confirmed with DR1-affinity assays. NEs prepared from mouse livers or Hepa1-6 cells, or *in vitro* synthesized proteins were incubated with DR1 oligonucleotides immobilized on streptavidin beads, and bound proteins were analyzed with immunoblotting. HNF-4 $\alpha$  synthesized *in vitro* or that in the NEs strongly bound to the resin, while SREBP-2 did not (Fig. S2C). These results further indicate that HNF-4 $\alpha$  but not SREBP-2 binds to the DR1 motif.

Consistently, the co-transfection of HNF-4 $\alpha$ -expressing plasmid increased the reporter activity of the *Cyp3a11* reporter construct containing the DR1 motif in HepG2 cells (Fig. S2D).

MOL #68577

Contribution of the DR1 motif to the SREBP-2-dependent suppression of *Cyp3a11* expression.

The contribution of the DR1 motif to the SREBP-2-mediated suppression of *Cyp3a11* expression was examined in reporter assays. The partial deletion of the DR1 motif or the introduction of mutations into the motif resulted in complete loss of the SREBP-2-mediated suppression in HepG2 (Fig. 4) and Hepa1-6 cells (data not shown). These results suggest that the DR1 motif is necessary for the SREBP-2-mediated suppression of *Cyp3a11* expression.

Interaction of SREBP-2 with HNF-4 $\alpha$  *in vitro*.

The obtained data suggested that SREBP-2 suppressed the HNF-4 $\alpha$ -mediated transcription of *Cyp3a11*. To test this possibility, we first performed GST pull-down assays to investigate the direct binding of SREBP-2 to HNF-4 $\alpha$ . *In vitro* synthesized SREBP-2, SREBP-2DN, SREBP-2DN-2 or SREBP-1a (Fig. 5A) was incubated with GST-fused HNF-4 $\alpha$  fragments (Fig. 5B) bound to beads. SREBP-2, SREBP-2DN and SREBP-2DN-2 interacted with GST-HNF-4 $\alpha$  (a) and the fragment (b) containing the DNA binding domain (DBD) but not with GST and other fragments (c, d, e) (Fig. 5C). These results suggest that SREBP-2 interacts with N-terminus of HNF-4 $\alpha$  (amino acids 1-129) containing DBD, through the region containing bHLH domain (amino acids 314-473). SREBP-1a interacted with HNF-4 $\alpha$  through the ligand

MOL #68577

binding domain (LBD) as reported previously (Fig. 5C) (Yamamoto et al., 2004).

To examine whether SREBP-2 could interact with HNF-4 $\alpha$  bound to the DR1 motif, DR1-affinity assays were performed. As shown in Fig. 5D, when HNF-4 $\alpha$  and SREBP-2 were mixed with the DR1 resin, only HNF-4 $\alpha$  (lane 3) but not SREBP-2 (lane 8) bound to the resin. Consistently, the addition of SREBP-2 did not affect the binding of HNF-4 $\alpha$  to DR1 probe in EMSAs (data not shown). These results suggest no formation of the ternary complex of SREBP-2-HNF-4 $\alpha$ -DR1. The results were further confirmed with GST pull-down assay. The binding of *in vitro* synthesized SREBP-2 to GST-HNF-4 $\alpha$  was abolished by the addition of DR1 oligonucleotides but not mutated oligonucleotides (Fig. 5E-F). These results suggest that SREBP-2 is unable to associate with HNF-4 $\alpha$  bound to the DR1 motif.

SREBP-2 inhibition of the interaction between HNF-4 $\alpha$  and PGC-1 $\alpha$ .

Because SREBP-2 bound to free HNF-4 $\alpha$  (Fig. 5C) but not that bound to the DR1 motif (Fig. 5D-F), SREBP-2 could inhibit the HNF-4 $\alpha$ -mediated *Cyp3a11* transcription through a mechanism other than its direct binding to HNF-4 $\alpha$ . Therefore, we hypothesized that SREBP-2 might affect the interaction between HNF-4 $\alpha$  and coactivators. To test this possibility, we performed GST pull-down assays with GST-HNF-4 $\alpha$ , *in vitro* synthesized SREBP-2 and PGC-1 $\alpha$ , a well-known coactivator for HNF-4 $\alpha$ . It was confirmed that PGC-1 $\alpha$  interacted with HNF-4 $\alpha$  in this system (Fig. 6A). As expected, the addition of SREBP-2



MOL #68577

attenuated the interaction between PGC-1 $\alpha$  and HNF-4 $\alpha$  (Fig. 6A). We then performed DR1-affinity assays using *in vitro* synthesized HNF-4 $\alpha$  and PGC-1 $\alpha$  with or without SREBP-2. PGC-1 $\alpha$  was associated with HNF-4 $\alpha$  bound to the DR1 resin (Fig. 6B and S3), and the interaction was attenuated in the presence of SREBP-2 (Fig. 6B, upper panel). On the other hand, SREBP-2 had no influence on the HNF-4 $\alpha$  binding to the resin (Fig. 6B, lower panel). These results suggest that SREBP-2 inhibits the interaction of PGC-1 $\alpha$  with HNF-4 $\alpha$  on the DR1 motif.

Next, the direct binding of SREBP-2 to PGC-1 $\alpha$  was tested in GST pull-down assays. As shown in Fig. 6C, SREBP-2 directly interacted with PGC-1 $\alpha$  in solution. The binding of GST-SREBP-2 to PGC-1 $\alpha$  was competed out with SREBP-2 but not SREBP-2DN (Fig. 6D). Finally, we performed co-immunoprecipitation assays with the liver NEs of LCD-fed mice using anti-SREBP-2 antibody. As shown in Fig. 6E, PGC-1 $\alpha$  was co-immunoprecipitated with SREBP-2. These results suggest that SREBP-2 directly interacts with PGC-1 $\alpha$  through its transactivation domain in mouse livers.

Role of PGC-1 $\alpha$  in the SREBP-2-mediated suppression of *Cyp3a11* expression.

Influence of PGC-1 $\alpha$  overexpression on the SREBP-2-mediated suppression of *Cyp3a11* expression was examined in reporter assays (Fig. 7A). The co-transfection of PGC-1 $\alpha$  expression plasmid increased reporter activity (lane 4 vs. lane 1), and SREBP-2 overexpression reduced reporter activities both in the

MOL #68577

absence (lane 2 vs. 1) and presence (lane 5 vs. lane 4) of co-expressed PGC-1 $\alpha$ . Intriguingly, the transfection of increasing amounts of PGC-1 $\alpha$  expression plasmid rescued the SREBP-2-mediated suppression (lanes 3 and 6 vs. lanes 2 and 5, respectively). To investigate the role of transactivation domain of SREBP-2 in the suppression of *Cyp3a11* expression, reporter assays were performed with SREBP-2 and SREBP-2DN expression plasmids. As expected from the results obtained in Fig. 6D, the deletion of the transactivation domain of SREBP-2 completely eliminated its suppressive effect on the *Cyp3a11* expression (Fig. 7B). Taken together, these results suggest that the interaction with PGC-1 $\alpha$  is necessary for the suppressive effect of SREBP-2 on the *Cyp3a11* expression.

Influence of dietary cholesterol levels on PGC-1 $\alpha$  binding to HNF-4 $\alpha$  on the DR1 motif.

To verify whether dietary cholesterol levels affected PGC-1 $\alpha$  binding to HNF-4 $\alpha$  in a genomic context, chromatin immunoprecipitation (ChIP) assays were performed with livers of CD- or LCD-fed mice (Fig. 8). *Pck1* (PEPCK1) and *Ldlr* promoters, containing known HNF-4 $\alpha$  and SREBP-2 binding motifs, respectively (Bennett et al., 2008; Miao et al., 2006), were also monitored as positive controls. The specific binding of HNF-4 $\alpha$  to the DR1-containing region (-1605 to -1464), but not to the negative control region (+4296 to +4543), of *Cyp3a11* was detected in the liver of both mice and the intensity was comparable (Fig. 8, left panels). Similar results were obtained for the *Pck1* promoter. In contrast, the

MOL #68577

specific binding of PGC-1 $\alpha$  to the *Cyp3a11* was clearly detected in the liver of CD-fed mice but was barely detected in the liver of LCD-fed mice (Fig. 8, right panels) despite that PGC-1 $\alpha$  protein levels in the liver nucleus of LCD-fed mice were 3.5 times higher than those of CD-fed mice (data not shown). As expected from the results shown above, no specific binding of SREBP-2 to the DR1-containing region of *Cyp3a11* was detected, whereas it bound to the *Ldlr* promoter, and the extent of the binding was higher in the liver of LCD-fed mice than in that of CD-fed mice. These results suggest that under conditions with reduced nutritional intake of cholesterol, the binding of PGC-1 $\alpha$ , but not HNF-4 $\alpha$ , to the DR1 motif in the *Cyp3a11* promoter is reduced in mouse livers.

MOL #68577

## Discussion

In this study, we found that limited supply of cholesterol resulted in the down-regulation of *Cyp3a11* expression in mouse livers. To understand the molecular mechanism of this phenomenon, we have investigated the role of SREBP-2 in the hepatic *Cyp3a11* expression. Present results demonstrate that the activation of SREBP-2 in mouse livers at limited cholesterol intake results in the down-regulation of *Cyp3a11* expression through a novel crosstalk of SREBP-2 and HNF-4 $\alpha$  involving PGC-1 $\alpha$ . SREBP-2 interacted with PGC-1 $\alpha$  *in vitro* (Fig. 6C-E) through its transactivation domain (Fig. 6D), which was necessary for the suppression of *Cyp3a11* expression in reporter assays (Fig. 7B). This SREBP-2 binding was suggested to inhibit the interaction of PGC-1 $\alpha$  with HNF-4 $\alpha$  *in vitro* (Fig. 6A-B). Consistently, DR1, the newly identified HNF-4 $\alpha$  binding motif of *Cyp3a11*, was necessary for the SREBP-2-mediated suppression of *Cyp3a11* expression in reporter assays (Fig. 4). Moreover, the binding of PGC-1 $\alpha$  to the DR1 motif in the *Cyp3a11* promoter was reduced under an SREBP-2-activated condition, although activated SREBP-2 had no influence on the HNF-4 $\alpha$  binding to the motif both *in vitro* and *in vivo* (Fig. 6B and 8). Finally, the overexpression of PGC-1 $\alpha$ , but not HNF-4 $\alpha$ , completely rescued the SREBP-2-mediated suppression of *Cyp3a11* expression (Fig. 7A and unpublished results). Taken together, it is suggested that activated SREBP-2 inhibits the interaction between HNF-4 $\alpha$  and PGC-1 $\alpha$ , reducing the HNF-4 $\alpha$ -mediated transactivation of *Cyp3a11*.

MOL #68577

We have found for the first time that SREBP-2 suppresses the HNF-4 $\alpha$ -mediated gene expression. Although SREBP-1 has been reported to inhibit the HNF-4 $\alpha$ -mediated gene expression (Ponugoti et al., 2007; Yamamoto et al., 2004), the mechanism of SREBP2-mediated transcriptional suppression is likely to differ from that by SREBP-1 in two points. First, SREBP-2 did not interact with HNF-4 $\alpha$  bound to DNA (Fig. 5D-F), while SREBP-1 directly interacted with HNF-4 $\alpha$  bound to the promoters of the target genes such as *Cyp7a1* and *Pck1* (Ponugoti et al., 2007; Yamamoto et al., 2004). Second, SREBP-2 directly interacted with PGC-1 $\alpha$  *in vitro* (Fig. 6C-D), while SREBP-1 did not interact with PGC-1 $\alpha$  (Yamamoto et al., 2004). Instead, SREBP-1 competed with PGC-1 $\alpha$  for the binding to HNF-4 $\alpha$  (Ponugoti et al., 2007; Yamamoto et al., 2004). Thus, our data clearly indicate that SREBP-2 down-regulates the HNF-4 $\alpha$ -mediated gene expression through a mechanism different from that for SREBP-1, involving the direct interaction with PGC-1 $\alpha$ .

PGC-1 $\alpha$  is reported to be crucial for the transcription mediated by other nuclear receptors, including CAR and PXR (Li and Chiang, 2005; Shiraki et al., 2003), as well as by HNF-4 $\alpha$ . Indeed, ligand-activated CAR and PXR have been shown to suppress the HNF-4 $\alpha$ -mediated transactivation by sequestering the common coactivator PGC-1 $\alpha$  (Bhalla et al., 2004; Li and Chiang, 2005; Miao et al., 2006). The increase in CAR/PGC-1 $\alpha$  or PXR/PGC-1 $\alpha$  complex formation and the concomitant decrease in HNF-4 $\alpha$ /PGC-1 $\alpha$  formation lead to the suppression of *Cyp7a1* and *Pck1* expression (Bhalla et al., 2004; Li and Chiang,

MOL #68577

2005; Miao et al., 2006). Therefore, it is of great interest to investigate in future studies whether hepatic gene transcriptions involving PGC-1 $\alpha$ , in addition to that of *Cyp3a11*, are also down-regulated under the condition with reduced cholesterol intake where SREBP-2 is activated.

Recent studies have demonstrated that transactivation by HNF-4 $\alpha$  requires the formation of a complex with coactivators, such as PGC-1 $\alpha$ , glucocorticoid receptor interacting protein-1 and steroid receptor coactivator-1 (Miao et al., 2006; Rhee et al., 2003; Wang et al., 1998). At present, it remains unknown whether SREBP-2 interacts with coactivators other than PGC-1 $\alpha$ . Future studies may help to understand the specificity for the interaction of SREBP-2 with coactivators.

HNF-4 $\alpha$  is reported to be crucial for the constitutive expression of several hepatic genes involved in lipid homeostasis and drug metabolism (Gonzalez, 2008; Jiang et al., 1995). In the present study, we have found that HNF-4 $\alpha$  transactivates *Cyp3a11* through the DR1 motif. Reporter assays demonstrated that *Cyp3a11* reporter constructs lacking the motif or having a mutation in the motif showed drastically reduced constitutive expression (Fig. 4). EMSAs, DR1-affinity assays and ChIP assays demonstrated that HNF-4 $\alpha$  bound to the DR1 motif in *Cyp3a11* both *in vitro* and *in vivo* (Fig. 3C, 8, S2A and S2C). Recent studies using HNF-4 $\alpha$  antisense RNA or the recombinant adenovirus that expresses HNF-4 $\alpha$ -small interfering RNA have demonstrated that HNF-4 $\alpha$  is critical for the *CYP3A4* expression in human hepatocytes (Jover et al., 2001; Kamiyama et al., 2007), which is consistent with our present results

MOL #68577

showing that HNF-4 $\alpha$  is involved in the constitutive expression of *Cyp3a11*.

CYP3A4 plays a crucial role in the xenobiotic metabolism, mediating the oxidation of more than 50% of clinically used therapeutic drugs (Eichelbaum and Burk, 2001; Gonzalez, 1992). In addition to xenobiotic metabolism, it also catalyzes the oxidation of steroid hormones such as testosterone and estradiol (Maenpaa et al., 1993; Stresser and Kupfer, 1997). Recently, CYP3A4 has been reported to mediate the conversion of cholesterol into 4 $\beta$ -hydroxycholesterol, an endogenous oxysterol found in the human circulation (Bodin et al., 2002; Bodin et al., 2001), and to be involved in the bile acid synthesis (Goodwin et al., 2003; Honda et al., 2001; Pikuleva, 2006). These findings imply that CYP3A enzymes are of importance in the cholesterol metabolism as well as xenobiotic metabolism. In the present study, we have demonstrated that hepatic *Cyp3a11* expression is reduced under the condition with reduced nutritional intake of cholesterol through an SREBP-2-mediated mechanism. This decreased expression of *Cyp3a11* may be a physiological response to maintain hepatic cholesterol level, corroborating the role of CYP3A enzymes in cholesterol homeostasis.

MOL #68577

Molecular Pharmacology Fast Forward. Published on October 6, 2010 as DOI: 10.1124/mol.110.068577  
This article has not been copyedited and formatted. The final version may differ from this version.

## Acknowledgment

We thank Dr. Anastasia Kralli (The Scripps Research Institute, La Jolla, CA) for her generous gift of pcDNA3/HA-hPGC-1 $\alpha$ , and Noriaki Yoda, Dr. Takayoshi Toriyabe and Kiwamu Aramiya (Tohoku University, Sendai, Japan) for excellent technical assistance and discussion.



## Author Contributions

*Participated in research design:* Shin-ichi Inoue, Kouichi Yoshinari and Yasushi Yamazoe.

*Conducted experiments:* Shin-ichi Inoue, Kouichi Yoshinari and Mika Sugawara.

*Performed data analysis:* Shin-ichi Inoue, Kouichi Yoshinari, Mika Sugawara and Yasushi

Yamazoe.

*Wrote or contributed to the writing of the manuscript:* Shin-ichi Inoue, Kouichi Yoshinari and

Yasushi Yamazoe.

## References

Bennett MK, Seo YK, Datta S, Shin DJ and Osborne TF (2008) Selective binding of sterol regulatory element-binding protein isoforms and co-regulatory proteins to promoters for lipid metabolic genes in liver. *J Biol Chem* 283(23):15628-15637.

Bhalla S, Ozalp C, Fang S, Xiang L and Kemper JK (2004) Ligand-activated pregnane X receptor interferes with HNF-4 signaling by targeting a common coactivator PGC-1alpha. Functional implications in hepatic cholesterol and glucose metabolism. *J Biol Chem* 279(43):45139-45147.

Bodin K, Andersson U, Rystedt E, Ellis E, Norlin M, Pikuleva I, Eggertsen G, Bjorkhem I and Diczfalusy U (2002) Metabolism of 4 beta -hydroxycholesterol in humans. *J Biol Chem* 277(35):31534-31540.

Bodin K, Bretillon L, Aden Y, Bertilsson L, Broome U, Einarsson C and Diczfalusy U (2001) Antiepileptic drugs increase plasma levels of 4beta-hydroxycholesterol in humans: evidence for involvement of cytochrome p450 3A4. *J Biol Chem* 276(42):38685-38689.

Brown MS and Goldstein JL (1997) The SREBP pathway: regulation of cholesterol metabolism by proteolysis of a membrane-bound transcription factor. *Cell* 89(3):331-340.

Eichelbaum M and Burk O (2001) CYP3A genetics in drug metabolism. *Nat Med* 7(3):285-287.

Gonzalez FJ (1992) Human cytochromes P450: problems and prospects. *Trends*

*Pharmacol Sci* 13(9):346-352.

Gonzalez FJ (2008) Regulation of hepatocyte nuclear factor 4 alpha-mediated

transcription. *Drug Metab Pharmacokinet* 23(1):2-7.

Goodwin B, Gauthier KC, Umetani M, Watson MA, Lochansky MI, Collins JL,

Leitersdorf E, Mangelsdorf DJ, Kliewer SA and Repa JJ (2003) Identification of bile acid

precursors as endogenous ligands for the nuclear xenobiotic pregnane X receptor. *Proc Natl*

*Acad Sci U S A* 100(1):223-228.

Harris RZ, Jang GR and Tsunoda S (2003) Dietary effects on drug metabolism and

transport. *Clin Pharmacokinet* 42(13):1071-1088.

Honda A, Salen G, Matsuzaki Y, Batta AK, Xu G, Leitersdorf E, Tint GS, Erickson SK,

Tanaka N and Shefer S (2001) Side chain hydroxylations in bile acid biosynthesis catalyzed by

CYP3A are markedly up-regulated in Cyp27<sup>-/-</sup> mice but not in cerebrotendinous xanthomatosis.

*J Biol Chem* 276(37):34579-34585.

Horton JD, Goldstein JL and Brown MS (2002) SREBPs: activators of the complete

program of cholesterol and fatty acid synthesis in the liver. *J Clin Invest* 109(9):1125-1131.

Jiang G, Nepomuceno L, Hopkins K and Sladek FM (1995) Exclusive

homodimerization of the orphan receptor hepatocyte nuclear factor 4 defines a new subclass of

nuclear receptors. *Mol Cell Biol* 15(9):5131-5143.

Jover R, Bort R, Gomez-Lechon MJ and Castell JV (2001) Cytochrome P450 regulation by hepatocyte nuclear factor 4 in human hepatocytes: a study using adenovirus-mediated antisense targeting. *Hepatology* 33(3):668-675.

Kamiyama Y, Matsubara T, Yoshinari K, Nagata K, Kamimura H and Yamazoe Y (2007) Role of human hepatocyte nuclear factor 4alpha in the expression of drug-metabolizing enzymes and transporters in human hepatocytes assessed by use of small interfering RNA. *Drug Metab Pharmacokinet* 22(4):287-298.

Li T and Chiang JY (2005) Mechanism of rifampicin and pregnane X receptor inhibition of human cholesterol 7 alpha-hydroxylase gene transcription. *Am J Physiol Gastrointest Liver Physiol* 288(1):G74-84.

Maenpaa J, Pelkonen O, Cresteil T and Rane A (1993) The role of cytochrome P450 3A (CYP3A) isoform(s) in oxidative metabolism of testosterone and benzphetamine in human adult and fetal liver. *J Steroid Biochem Mol Biol* 44(1):61-67.

Miao J, Fang S, Bae Y and Kemper JK (2006) Functional inhibitory cross-talk between constitutive androstane receptor and hepatic nuclear factor-4 in hepatic lipid/glucose metabolism is mediated by competition for binding to the DR1 motif and to the common coactivators, GRIP-1 and PGC-1alpha. *J Biol Chem* 281(21):14537-14546.

Miyata M, Nagata K, Yamazoe Y and Kato R (1995) Transcriptional elements directing a liver-specific expression of P450/6 beta A (CYP3A2) gene-encoding testosterone 6 beta-hydroxylase. *Arch Biochem Biophys* 318(1):71-79.

Monsalve M, Wu Z, Adelmant G, Puigserver P, Fan M and Spiegelman BM (2000) Direct coupling of transcription and mRNA processing through the thermogenic coactivator PGC-1. *Mol Cell* 6(2):307-316.

Pikuleva IA (2006) Cytochrome P450s and cholesterol homeostasis. *Pharmacol Ther* 112(3):761-773.

Ponugoti B, Fang S and Kemper JK (2007) Functional interaction of hepatic nuclear factor-4 and peroxisome proliferator-activated receptor-gamma coactivator 1alpha in CYP7A1 regulation is inhibited by a key lipogenic activator, sterol regulatory element-binding protein-1c. *Mol Endocrinol* 21(11):2698-2712.

Puigserver P, Adelmant G, Wu Z, Fan M, Xu J, O'Malley B and Spiegelman BM (1999) Activation of PPARgamma coactivator-1 through transcription factor docking. *Science* 286(5443):1368-1371.

Rhee J, Inoue Y, Yoon JC, Puigserver P, Fan M, Gonzalez FJ and Spiegelman BM (2003) Regulation of hepatic fasting response by PPARgamma coactivator-1alpha (PGC-1): requirement for hepatocyte nuclear factor 4alpha in gluconeogenesis. *Proc Natl Acad Sci U S A*

100(7):4012-4017.

Shimada T, Yamazaki H, Mimura M, Inui Y and Guengerich FP (1994) Interindividual variations in human liver cytochrome P-450 enzymes involved in the oxidation of drugs, carcinogens and toxic chemicals: studies with liver microsomes of 30 Japanese and 30 Caucasians. *J Pharmacol Exp Ther* 270(1):414-423.

Shiraki T, Sakai N, Kanaya E and Jingami H (2003) Activation of orphan nuclear constitutive androstane receptor requires subnuclear targeting by peroxisome proliferator-activated receptor gamma coactivator-1 alpha. A possible link between xenobiotic response and nutritional state. *J Biol Chem* 278(13):11344-11350.

Stresser DM and Kupfer D (1997) Catalytic characteristics of CYP3A4: requirement for a phenolic function in ortho hydroxylation of estradiol and mono-O-demethylated methoxychlor. *Biochemistry* 36(8):2203-2210.

Toriyabe T, Nagata K, Takada T, Aratsu Y, Matsubara T, Yoshinari K and Yamazoe Y (2009) Unveiling a new essential cis element for the transactivation of the CYP3A4 gene by xenobiotics. *Mol Pharmacol* 75(3):677-684.

Vega RB, Huss JM and Kelly DP (2000) The coactivator PGC-1 cooperates with peroxisome proliferator-activated receptor alpha in transcriptional control of nuclear genes encoding mitochondrial fatty acid oxidation enzymes. *Mol Cell Biol* 20(5):1868-1876.

Wang JC, Stafford JM and Granner DK (1998) SRC-1 and GRIP1 coactivate transcription with hepatocyte nuclear factor 4. *J Biol Chem* 273(47):30847-30850.

Wilkinson GR (1997) The effects of diet, aging and disease-states on presystemic elimination and oral drug bioavailability in humans. *Adv Drug Deliv Rev* 27(2-3):129-159.

Wiwi CA, Gupte M and Waxman DJ (2004) Sexually dimorphic P450 gene expression in liver-specific hepatocyte nuclear factor 4alpha-deficient mice. *Mol Endocrinol* 18(8):1975-1987.

Wolbold R, Klein K, Burk O, Nussler AK, Neuhaus P, Eichelbaum M, Schwab M and Zanger UM (2003) Sex is a major determinant of CYP3A4 expression in human liver. *Hepatology* 38(4):978-988.

Yamamoto T, Shimano H, Nakagawa Y, Ide T, Yahagi N, Matsuzaka T, Nakakuki M, Takahashi A, Suzuki H, Sone H, Toyoshima H, Sato R and Yamada N (2004) SREBP-1 interacts with hepatocyte nuclear factor-4 alpha and interferes with PGC-1 recruitment to suppress hepatic gluconeogenic genes. *J Biol Chem* 279(13):12027-12035.

Yoon JC, Puigserver P, Chen G, Donovan J, Wu Z, Rhee J, Adelmant G, Stafford J, Kahn CR, Granner DK, Newgard CB and Spiegelman BM (2001) Control of hepatic gluconeogenesis through the transcriptional coactivator PGC-1. *Nature* 413(6852):131-138.

Yoshinari K, Takagi S, Yoshimasa T, Sugatani J and Miwa M (2006) Hepatic CYP3A

MOL #68577

Molecular Pharmacology Fast Forward. Published on October 6, 2010 as DOI: 10.1124/mol.110.068577  
This article has not been copyedited and formatted. The final version may differ from this version.

expression is attenuated in obese mice fed a high-fat diet. *Pharm Res* 23(6):1188-1200.

Yoshinari K, Yoda N, Toriyabe T and Yamazoe Y (2010) Constitutive androstane receptor transcriptionally activates human CYP1A1 and CYP1A2 genes through a common regulatory element in the 5'-flanking region. *Biochem Pharmacol* 79(2):261-269.



MOL #68577

Molecular Pharmacology Fast Forward. Published on October 6, 2010 as DOI: 10.1124/mol.110.068577  
This article has not been copyedited and formatted. The final version may differ from this version.

## Footnotes

This work was supported in part by Grant-in-Aid from Ministry of Health, Labor, and Welfare  
of Japan and Ministry of Education, Culture, Sports, Sciences and Technology of Japan  
[22659028].

## Legends to Figures

Fig. 1. Influence of dietary cholesterol level on the hepatic expression of *Cyp3a11* and SREBP-2-responsive genes.

Mice were fed CD, LCD or 2% cholesterol-supplemented LCD for 6 days. A, Hepatic mRNA levels were determined by quantitative reverse transcription-PCR. mRNA levels were normalized by those of  *$\beta$ -actin*, and those in CD-fed mice are set at 1. Data are the mean  $\pm$  S.D. (n=6-7). \*, P < 0.05, \*\*, P < 0.01. *Srebf2*, *Ldlr*, *Hmgcs1* and *Sqle* encode SREBP-2, LDL-R, 3-hydroxy-3-methylglutaryl-CoA synthase 1 and squalene epoxidase, respectively. B, Mouse liver NEs (100  $\mu$ g) and *in vitro* synthesized nuclear form of SREBP-2 were subjected to immunoblotting with 8% SDS-polyacrylamide gel and anti-SREBP-2 antibody. Molecular weight markers are shown on the left. The arrows indicate the bands corresponding to SREBP-2, whose intensities were quantified using NIH image software.

Fig. 2. Identification of a region responsible for the SREBP-2-dependent suppression of *Cyp3a11* expression.

HepG2 cells were transfected with pSV- $\beta$ -galactosidase Control Vector (1  $\mu$ g) and each reporter construct (1  $\mu$ g) shown on the left in the presence of either empty plasmid (open bars) or expression plasmid of hSREBP-2 nuclear form (closed bar) (0.5  $\mu$ g each), and reporter activities

were determined as described under Materials and Methods. Luciferase activities were normalized with  $\beta$ -galactosidase activities and are shown as ratios to those in control cells for each construct. The numbers in parentheses represent ratios of the activity to those in the cells transfected with pGL4.10 and empty expression plasmid. The numbers above the constructs represent the positions from the *Cyp3a11* transcriptional starting point. Data are the mean  $\pm$  S.D. (n=4). Results shown are representative of three independent assays.

Fig. 3. Binding of HNF-4 $\alpha$  to the DR1 motif in *Cyp3a11*.

A, Nucleotide sequence of the region from -1581 to -1524 of *Cyp3a11* is shown. Putative HNF-4 $\alpha$  binding motif DR1 is shown in bold with arrows. B, The sequences of oligonucleotides used in EMSAs are shown. DR1 and mutated DR1 are shown in bold. Mutated nucleotides are underlined. C, EMSAs were performed as described under Materials and Methods with radiolabeled oligonucleotides and *in vitro* synthesized HNF-4 $\alpha$ . SS represents the supershifted complex with anti-HNF-4 $\alpha$  antibody.

Fig. 4. Contribution of the DR1 motif to the SREBP-2-dependent suppression of *Cyp3a11* expression.

Schematic structures of luciferase reporter gene constructs are shown on the left and a shaded

box represents the DR1 motif. In the top construct, the motif was mutated as in Fig. 3B.

Reporter assays were performed with HepG2 cells and results are shown as in Fig. 2.

#### Fig. 5. Interaction of SREBP-2 with HNF-4 $\alpha$ .

Schematic structures of SREBP-2, SREBP-2 mutants and SREBP-1a (A) and of HNF-4 $\alpha$  and its deletion mutants (B) are shown. TA: transactivation domain. C, GST pull-down assays were performed as described under Materials and Methods. GST or GST-HNF-4 $\alpha$  bound to beads was incubated with *in vitro* synthesized SREBP-2, SREBP-2DN, SREBP-2DN-2 or SREBP-1a. Proteins bound to the resin were subjected to immunoblotting with 8% (SREBP-2 and SREBP-1a), 10% (SREBP-2DN) or 15% (SREBP-2DN-2) SDS-polyacrylamide gels and anti-SREBP-2 or anti-SREBP-1a antibody. D, DR1-affinity assays were performed as described under Materials and Methods with *in vitro* synthesized HNF-4 $\alpha$  and SREBP-2. Eluates, unbound fractions and input samples were subjected to immunoblotting with 8% SDS-polyacrylamide gel and anti-HNF-4 $\alpha$  or anti-SREBP-2 antibody. E and F, GST pull-down assays were performed. GST or GST-HNF-4 $\alpha$  bound to beads were incubated with *in vitro* synthesized SREBP-2 and various amounts of double-stranded DR1 or DR1mt oligonucleotides (+, 40 pmol; ++, 133 pmol; +++, 400 pmol) shown in Fig. 3B. SREBP-2 bound to GST-HNF-4 $\alpha$  was subjected to immunoblotting with 8% SDS-polyacrylamide gel and

anti-SREBP-2 antibody.

Fig. 6. Influence of SREBP-2 on the interaction between HNF-4 $\alpha$  and PGC-1 $\alpha$ .

A, C and D, GST pull-down assays were performed as described under Materials and Methods.

GST or GST-HNF-4 $\alpha$  bound to beads was incubated with *in vitro* synthesized PGC-1 $\alpha$  in the

absence or presence of SREBP-2 (A). GST or GST-SREBP-2 bound to beads was incubated

with *in vitro* synthesized PGC-1 $\alpha$  (C and D). In D, various amounts of *in vitro* synthesized

SREBP-2 or SREBP-2DN were mixed with GST-SREBP-2 before the addition of PGC-1 $\alpha$ .

PGC-1 $\alpha$  bound to GST-HNF-4 $\alpha$  or GST-SREBP-2 was subjected to immunoblotting with 8%

SDS-polyacrylamide gel and anti-PGC-1 $\alpha$  antibody. B, DR1-affinity assays were performed as

described under Materials and Methods with *in vitro* synthesized HNF-4 $\alpha$  and PGC-1 $\alpha$  with or

without SREBP-2. A portion of input proteins (upper, 37.5%; lower, 50%) were also subjected.

The eluates with 0.5 M NaCl solution were subjected to immunoblotting with 8%

SDS-polyacrylamide gel and anti-HNF-4 $\alpha$  or anti-PGC-1 $\alpha$  antibody. E,

Co-immunoprecipitation assays were performed with liver NEs prepared from mice fed LCD

for 6 days using control IgG or anti-SREBP-2 antibody as described under Materials and

Methods. The immunoprecipitated samples, NEs (50  $\mu$ g) and *in vitro* synthesized proteins were

subjected to immunoblotting with 8% SDS-polyacrylamide gel and anti-SREBP-2 and

anti-PGC-1 $\alpha$  antibody. Molecular weight markers are shown on the left and the arrows indicate the bands corresponding to SREBP-2 or PGC-1 $\alpha$ .

Fig. 7. Role of the interaction of SREBP-2 with PGC-1 $\alpha$  in the suppression of *Cyp3a11* expression.

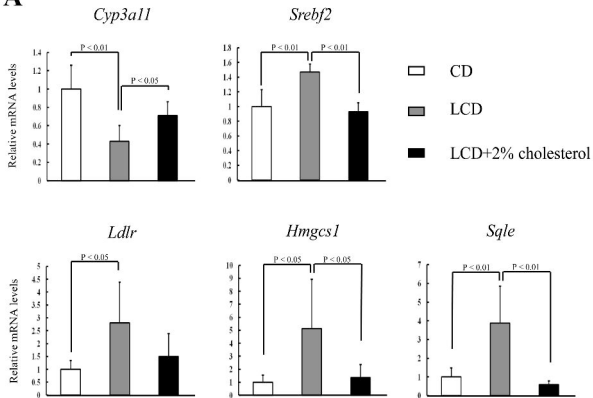
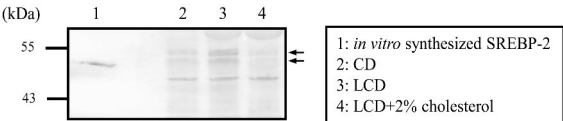
Reporter assays were performed with pSV- $\beta$ -galactosidase Control Vector (1  $\mu$ g), the reporter construct shown (1  $\mu$ g) in combination with hSREBP-2 expression plasmid (0.3  $\mu$ g), and various amounts (0.1, 0.5, 1  $\mu$ g) of PGC-1 $\alpha$  expression plasmid (A), or empty (Control, 0.5  $\mu$ g), hSREBP-2 (0.5  $\mu$ g) or hSREBP-2DN (0.5  $\mu$ g) expression plasmid (B) in HepG2 cells.

Luciferase activities were normalized with  $\beta$ -galactosidase activities and the normalized activities in the cells transfected with *Cyp3a11* reporter construct were divided with those in the corresponding cells transfected with pGL4.10. The reporter activities in the cells transfected with empty plasmid are set at 1. Data are the mean  $\pm$  S.D. (n=4). Results shown are representative of three independent assays.

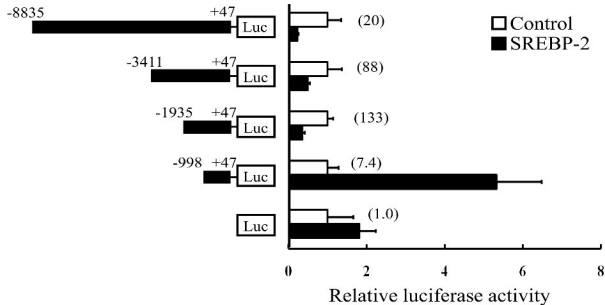
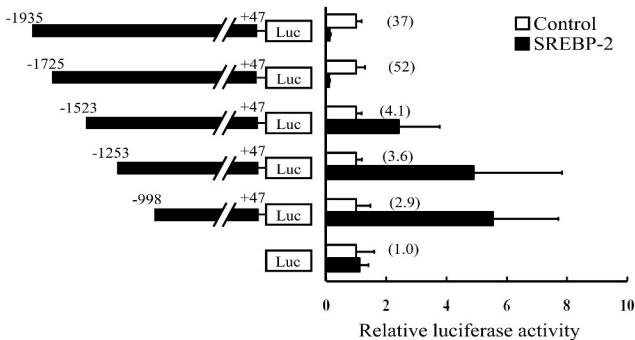
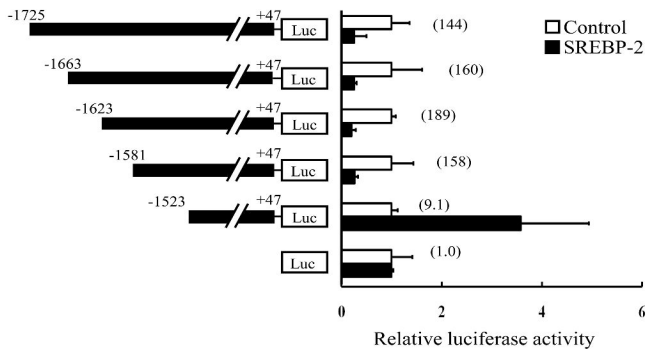
Fig. 8. Influence of dietary cholesterol levels on HNF-4 $\alpha$  and PGC-1 $\alpha$  binding to *Cyp3a11* promoter.

ChIP assays were performed with livers of mice fed CD or LCD for 6 days using antibodies

indicated as described under Materials and Methods. The immunoprecipitated DNA, along with the DNA isolated before immunoprecipitation (Input), were analyzed by PCR using specific primers (Table S7) for the indicated regions. Results shown are representative of three independent assays. NT, not tested.

**Fig. 1.****A****B**



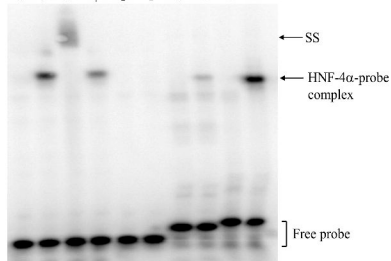
**Fig. 2.****A****B****C**

**Fig. 3.****A****B**

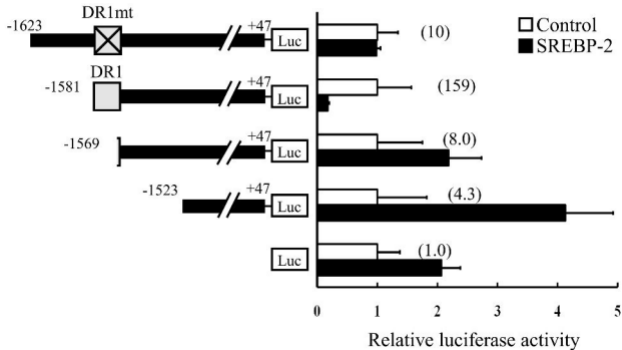
DR1 5'-TAATGAGGGCAAAGTTCTCAGG-3'  
 DR1mt 5'-TAATGAGTTACCCTTTCTCAGG-3'  
 CYP7A1 5'-TACCTGTGGACTTAGTTCAAGGCCAGTTACTA-3'  
 PEPCK1 5'-GAATTCCTTCTCATGACCTTTGGCCGTGGGAGTGA-3'  
 LDL-R 5'-GAAAATCACCCCACTGCAAA-3'

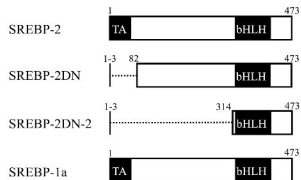
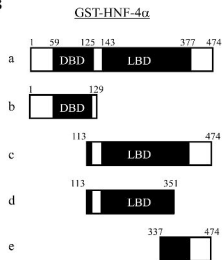
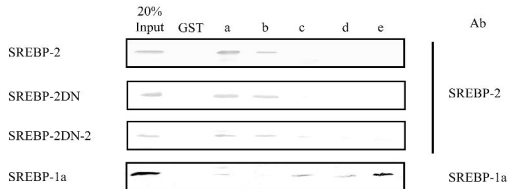
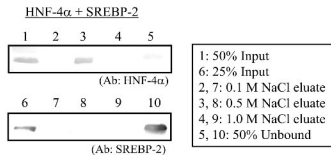
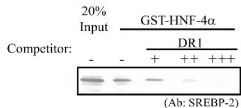
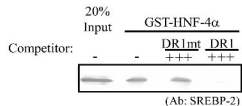
**C**

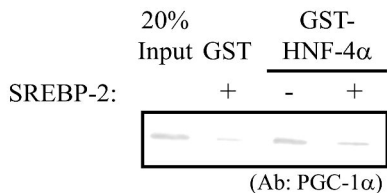
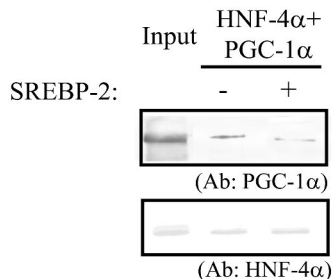
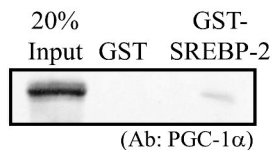
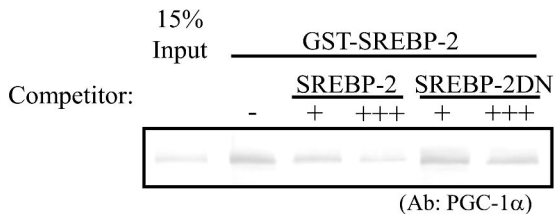
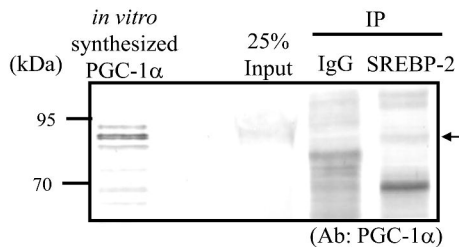
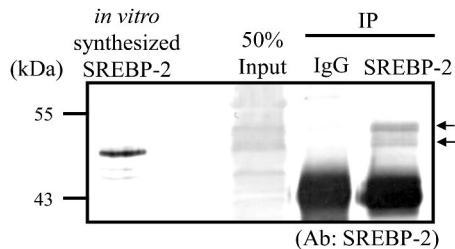
Probe:	DR1				DR1mt		CYP7A1		PEPCK1	
HNF-4 $\alpha$ :	-	+	+	+	-	+	-	+	-	+
HNF-4 $\alpha$ Ab:	-	-	+	-	-	-	-	-	-	-
IgG:	-	-	-	+	-	-	-	-	-	-

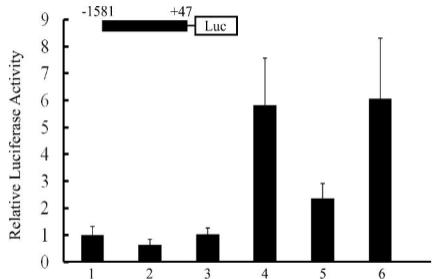


**Fig. 4.**

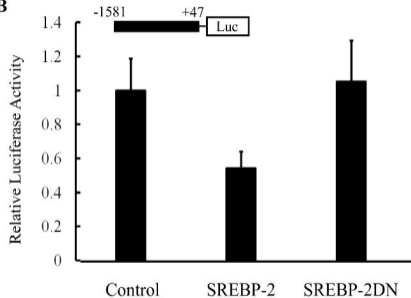


**Fig. 5.****A****B****C****D****E****F**

**Fig. 6.****A****B****C****D****E**

**Fig. 7.****A**

SREBP-2	-	300	300	-	300	300	(ng)
PGC-1 $\alpha$	-	-	100	500	500	1000	(ng)

**B**

Control	SREBP-2	SREBP-2DN
---------	---------	-----------

**Fig. 8.**